Archives of Microbiology (2024) 206:186
https://doi.org/10.1007/s00203-023-03780-w

ORIGINAL PAPER

Anti-fungal effects of novel *N*-(*tert*-butyl)-2-(pyridin-2-yl) imidazo[1,2-a]pyridin-3-amine derivative and it's in-vitro, in-silico, and mode of action against *Candida* spp.

Manivannan Nandhagopal[1] · Ramanjaneyulu Mala[2] · Kanagasabai Somarathinam[3] · Divya Dhakshinamurthy[4] · Mathivanan Narayanasamy[5] · Priyadharshni Vijayan[5] · Manimuthu Mani Shankar[6]

Received: 29 September 2023 / Revised: 21 November 2023 / Accepted: 28 November 2023 / Published online: 21 March 2024

Abstract

Imidazoles are a category of azole antifungals that encompass compounds such as ketoconazole, miconazole, esomeprazole, and clotrimazole. In contrast, the triazoles group, which includes fluconazole, voriconazole, and itraconazole, also plays a significant role. The rise of antibiotic resistance in fungal pathogens has evolved into a substantial global public health concern. In this study, two newly synthesized imidazo[1,2-a]pyridine derivative (Probe I and Probe II) molecules were investigated for its antimicrobial potency against of a panel of bacterial (Gram-positive and Gram-negative bacteria) and fungal pathogens. Among the different types of pathogens, we found that Probe II showed excellent antifungal activity against fungal pathogens, based on the preliminary screening the potent molecule further investigated against multidrug-resistance *Candida* sp. ($n = 10$) and compared with commercial molecules. In addition, in-silico molecular docking, its dynamics, absorption, distribution, metabolism, excretion and toxicity (ADMET) were analyzed. In this study, the small molecule (Probe II) displayed potent activity only against the *Candida* spp. including several multidrug-resistant *Candida* spp. Probe II exhibited minimum inhibitory concentration ranges from 4 to 16 µg/mL and minimum fungicidal concentration in the range 4−32 µg/mL as the lowest concentration enough to eliminate the *Candida* spp. The selected molecules inhibit the formation of yeast to mold as well as ergosterol formation by the computational simulation against Sterol 14-alpha demethylase (CYP51) and inhibition of ergosterol biosynthesis by in-vitro model show that the Probe II completely inhibits the formation of ergosterol in yeast cells at 2× MIC. The ADMET analysis Probe II could be moderately toxic to the human being, though the in-vitro toxicity studies will help to understand the real-time toxic level. The novel compound Probe II, which was synthesized during the study, shows promise for development into a new generation of drug treatments aimed at addressing the emerging drug resistance in *Candida* sp.

Keywords Drug development · Antifungal · Biological compatibility · Confocal microscopic observation

Abbreviations

ADMET	Absorption, distribution, metabolism, excretion and toxicity
AIDS	Acquired immune deficiency syndrome
MDR	Multi-drug resistance
MIC	Minimum inhibitory concentration
NA	Not appeared
ND	Not determined
NC	Negative control
PC	Positive control
ZOI	Zone of inhibition
MFC	Minimum fungicidal concentration
C1	*C. tropicalis* (ATCC750)
C2	*C. albicans* (KT315910)
C3	*C. tropicalis* (KT315910)
C4	*C. albicans* (KT315901)
C5	*C. albicans* (KT831886)
C6	*Candida* Sp. (KT831887)
C7	*C. dubliniensis* (KT831888)
C8	*C. albicans* (KT831889)
C9	*C. albicans* (KT315909)
Probe I	2-(3-(*Tert*-Butylamino)imidazo[1,2-*a*]pyridin-2-yl)phenol
Probe II	*N*-(*Tert*-Butyl)-2-(pyridin-2-yl)imidazo[1,2-*a*]pyridin-3-amine
MD	Molecular simulation

Communicated by Yusuf Akhter.

Extended author information available on the last page of the article

RMSD	Root mean square deviation
RMSF	Root mean square fluctuation
MHB	Muller Hinton broth
MHA	Muller Hinton agar
CLSI	Clinical & Laboratory Standards Institute
PBS	Phosphate buffer saline
PDB	Protein data bank

Introduction

The resistance of *Candida albicans* to azole drugs represents a great global challenge. The resistance of *C. albicans* to azole drugs represents a great global challenge (Cui et al. 2022). Fungal infection accounts for an annual estimate of 15 lakh deaths and causes infection over a billion (Mahmoud et al. 2021). Among the human pathogenic fungi, *Candida* genus is considered to be of great clinical vulnerable, and the genus *Candida* is pivotal in causing infection, including oral candidiasis, vaginitis, cutaneous candidiasis, candidemia, and systemic infections (Oliveira Santos et al. 2018; Alabi et al. 2023). *C. albicans* is an opportunistic second-most common pathogen (Bar-Yosef et al. 2017). Although *C. albicans* is generally considered to be harmless, it can occasionally result in serious infections that can be life-threatening (Mayer et al. 2013). The rise in candidemia caused by non-albicans *Candida* spp. and the increasing resistance to antifungal drugs is a growing interest in the medical field. The presence of fungi that are resistant to multiple drugs, such as *Candida auris* and other *Candida* spp., adds to the complexity of this issue. In hospitals, the prevalence of multidrug-resistant *Candida* species, *C. albicans* and *Candida glabrata*, poses a significant threat to immunocompromised individuals (Panda et al. 2021; Daneshnia et al. 2023). *Candida* infections in the bloodstream remain the most prevalent and serious fungal disease, and 70–80% of the *C. albicans* isolates discovered in sick patients are caused by *Candida spp.* (Chin et al. 2016). The *C. lusitaniae*, *C. krusei*, and *C. kefyr* are among the *Candida* spp. that have been reported to show resistance to multiple drugs in patients with hematologic malignancies after exposure to antifungals. They are the second-most commonly documented *Candida* spp. causing deep-seated infections in the US and several European centers (Wang et al. 2015; Zhao et al. 2015).

The mechanism of antifungal resistance in these species is primarily due to the overexpression of multidrug efflux pumps, alterations in target proteins, and modifications in the composition of the membrane sterol (Bruder-Nascimento et al. 2014). Likewise, the new emergence of *C. auris*, which is often resistant to available antifungal drugs, further aggravates the challenge of treating candidemia. The available antifungal drugs such as fluconazole and amphotericin B and other azole antifungal agents are often ineffective against *C. auris*, leaving echinocandins as the first-line drugs for treatment. However, the limited options for treating *C. auris* infections emphasize the urgent need for new antimycotic molecules with alternative modes of action against this pan-resistant *Candida* spp. (Kamli et al. 2021). The yeast cells become resistant to the many azole antifungal agents such as fluconazole, itraconazole, and ketoconazole which are the only azole antifungal agents available in nineteenth century. Since *Candida* spp. is highly life-threatening worldwide, there is an urgent need for novel chemotherapeutic molecules for treating widespread fungal infections (Rahimi-Verki et al. 2016; Odds 1993; Iyer et al. 2022). Therefore, a new imidazo[1,2-a]pyridine moiety has been found to be effective against the multiple *Candida* spp. Further, the biological compatibilities of this molecule were studied extensively.

Experimental section

Materials and methods

The newly synthesized imidazol[1,2-a]pyridine derivatives namely [Probe I (2-(3-(*tert*-butylamino)imidazo[1,2-a]pyridin-2yl) phenol)] and Probe II [(*N*-(*tert*-butyl)-2-(pyridin-2-yl)imidazo[1,2-a]pyridin-3-amine)] were obtained from the Department of organic chemistry, Council of Scientific and Industrial Research–Central Leather Research Institute (CSIR–CLRI), Chennai, Tamil Nadu and maintained at room temperature for further use.

Strain selection

Staphylococcus aureus (ATCC® 25923™), *Enterococcus faecalis* (ATCC® 29212™), *Escherichia coli* (ATCC® 11229™), *Pseudomonas aeruginosa* (ATCC® 15442™), *C. albicans* (ATCC® 10231™), and *C. albicans* (ATCC90028) were obtained from American Types of Culture Collection (ATCC) and eight clinical isolates of *Candida* spp. were obtained from Biocontrol Microbial Metabolites Lab, Centre for Advanced Studies in Botany, University of Madras, Guindy Campus, Chennai, with the GenBank submission numbers, namely *C. tropicalis* (ATCC750), *C. albicans* (KT315910), *C. tropicalis* (KT315910), *C. albicans* (KT315901), *C. albicans* (KT831886), *Candida* sp. (KT831887), *C. dubliniensis* (KT831888), *C. albicans* (KT831889), and *C. albicans* (KT315909).

Antibiotics preparation

The antifungal agents were procured from different medical shop near Kotturpuram, Chennai, Tamil Nadu, India, and every antibiotic were prepared according to its

manufacturing instructions using double-distilled water, dimethyl sulfoxide and methanol as a solvent with the following formula:

$$\text{Total weight/Potency} \times V \times C = W$$

where V is the volume required, C is the final concentration, and W is the weight of the tablet.

Antimicrobial activity

Antimicrobial activity of synthesized two imidazo[1,2-a] pyridine (Probes I and II) derivatives was initially screened for antimicrobial activities, and based on activities, the disk diffusion assay was carried out for 10 *Candida* spp. Briefly, the pathogens were harvested from the early stationary phase of growth, and cultures' concentration was adjusted to 0.4 O.D for bacteria and 0.5 (O.D) for *C. albicans* using sterile Muller Hinton Broth (MHB); the pathogens were swabbed on sterile Muller Hinton Agar (MHA) medium on Petri plates; the wells made using cork borer 100 µL of crude metabolites were loaded on the respective wells in a Petri plates for the disk diffusion assay 40 µg/disk concentration of probe 2 and commercially available antibiotics (Fluconazole, Esomeprazole and Ketoconazole) were loaded on disk and kept near MHA medium; every plate loaded with test samples was incubated at 37 °C for 16 h. The zone of inhibitions was measured using zone scale. Experiments were performed with biological triplicates.

Minimum inhibitory concentrations (MICs)

The MIC of Probes and commercial antibiotics were determined in 96-well micro-titer test plates. According to Clinical & Laboratory Standards Institute (CLSI) guidelines and EUCAST, the MIC was conducted. Test pathogens were cultured in MHB (HiMedia, India). Different concentration probe II (512, 256, 128, 64, 32, 16, 8, 4, 2, and 1 mg/L), Probe I (1819.75, 909.87, 454.93, 227.46, 113.73, 56.86, 28.43, 14.21, 7.10, and 3.55 µM/L) and Probe II (1922.35, 961.17, 480.58, 240.29, 120.14, 60.07, 30.03, 15.01, 7.50, and 3.75 µM/L) were added to the 96-well plates, and 5 µL of clinical pathogens (OD 0.4–0.5 at 600 nm) grown for 12 h was added to respective wells. After 16 h of incubation at 37 °C, the 10 µL of freshly prepared MTT (3-(4,5-Dimethylthiazol-2-yl)-2,5-Diphenyltetrazolium Bromide) (Sigma, USA) (5 mg/mL concentration) was added to all the wells including control; after being covered with aluminum foil, each plate was incubated for 30 min at dark condition. Then, 100 µL of Dimethyl Sulfoxide (DMSO) as a solubilizing agent was added and then kept for 15−30 mins. To determine the proportion of growth inhibition and to record it, optical density (OD) measurements were made at 595 nm in an ELISA reader. In addition, pathogens are compared with the antibiotics.

Minimum fungicidal concentration (MFC)

The minimum fungicidal concentration of Probe II was carried out for 10 fungal pathogens. Briefly a series of various concentration of molecules and antibiotics were tested at different concentration of 512, 256, 128, 64, 32, 16, 8, 4, 2, and 1 mg/L, and the molecular weight of test compound Probe I (1819.75, 909.87, 454.93, 227.46, 113.73, 56.86, 28.43, 14.21, 7.10, and 3.55 µM/L) and Probe II (1922.35, 961.17, 480.58, 240.29, 120.14, 60.07, 30.03, 15.01, 7.50, and 3.75 µM/L) was calculated. Imidazo molecules are dissolved in 96-well plates using (Sabouraud dextrose broth) SDB medium. The 5 µL of fungal pathogens was inoculated, then plates were incubated for 18 h. After incubation, the four wells were chosen before and after MIC values, and from all the wells, the 100 µL samples were transferred into sterile MHA medium and spread using L road; after 24 h incubation, the plates and existence of colonies were observed and the absence of colonies were noted as minimum fungicidal concentration and results were noted.

Hemolytic assays

The biological compatibility of Probe II was carried out using human blood cells. The freshly collected human blood cells from the voluntaries were washed thrice with PBS. The different concentrations of imidazo molecule (512, 256, 128, 64, 32, 16, 8, 4, 2, and 1 µg/mL) were diluted in 800 µL of PBS solution, and 200 µL of blood sample was added to each micro-centrifuge tubes separately and sterilized microfilter plates were used after the tubes were centrifuged at 5000 rpm for 7 mins and incubated for 1 hr at 37 °C. Absorbance measurements were taken at 570 nm and the amount of hemoglobin were calculated. The PBS was used as the negative control and 1% Triton X-100 was used as a positive control. The % hemolysis was interpreted as follows:

$$\text{Hemolysis Percentage} = \left(A_{540}\text{ of extract}\right) - \left(A_{540}\text{ of PBS}\right) / \left[\left(A_{540}\text{ of 1\% Triton x - 100}\right)\left(A_{540}\text{ of PBS}\right)\right] \times 100$$

These investigations were done twice and results are expressed by mean ± standard deviation (± SD).

Live and dead assay

Live and dead fungal (*Candida* spp.) viability assay of Probe II was analyzed using the modified technique of Velusamy and coworkers (2015). Briefly, the 20-h-old fungal culture grown in SDB was diluted as optical density (O.D) 0.4 at

600 nm and 2× MIC of Probe II was treated with selected *C. albicans* for 25 mL, the cells were incubated at 37 °C and 1 mL of cultured broth was transferred into sterile microcentrifuge tubes for different time period ranging from 0 min to 6 h. The suspended cells were separated by centrifuging for 10 mins at 7000 rpm, and 0.1% of Acridine orange and ethidium bromide (1:1) was added to the pellet mixed well and 0.5 mL of PSB pH-7.0 was added to each pellet and centrifuge 7000 rpm. After discarding supernatants, pellets were again dissolved in 50 µL PBS solution, and one drop of cell suspension was placed in a microscopic slide covered with a cover slip and observed under the Multiphoton Confocal Microscope 600 magnification. The number of cells dead was calculated, and the inhibition of yeast to mold formation was also observed.

Molecular docking and dynamics

Structure preparations

The molecule Probe II was docked against the Sterol 14-alpha demethylase (CYP51) protein from *C. albicans* using the AutoDock 4.2 tool. The 3D crystal structures of CYP51 (PDB ID: 5TZ1) were downloaded from the Protein Data Bank (PDB) and constructed for future investigations. The 3D structures of CYP51 were applied to remove the water molecules and added to the charges by Pymol software. The structure of Probe II (ligand) was drawn in Chemdraw Ultra and then exported as a PDB file using Open Babel. The structure of the ligand was energy-minimized to stabilize. The Probe II energy minimization was carried out in Avogadro software. For energy minimization, the chemical force field and steepest descent algorithm were applied (Somarathinam et al. 2023).

Molecular docking simulations

The AutoDock 4.2 docking program57 employed the optimized CYP51 protein and Probe II (ligand). Partial Lollman charges and polar hydrogen atoms were sent to CYP51 target receptors, which were then converted into "pdbqt" file that contains solvation parameter coordinates and partial charges. In addition, the ligand was given hydrogen atoms and all the torsion angles were being transformed into a "pdbqt." To create grid maps surrounding the active site, an Autogrid box of coordinates with 40 40 40 points and a grid spacing of 0.375 was created. The Lamarckian genetic algorithm was utilized, and the default docking parameters were adjusted for a total of 100 GA runs. With respect to substantial interaction of H-bond with binding energy (kcal/mol), least root mean square deviation (RMSD), and inhibitory concentration, the result for docking of protein–ligand complexes was examined from the top clusters (Somarathinam et al. 2023).

Molecular dynamics (MD) simulations

The characteristics of protein and ligand complexes can be thoroughly understood via MD simulations, using the GROMACS 2018.3 programme, and it was carried as proposed by Somarathinam et al. (2023) with slight modification. Briefly, MD up to 100 ns was performed on the Probe II–CYP51 complex. Proteins, ligands and H_2O were employed as parts of MD. Protein chains (in apo state) of all four complexes were segregated and along with its topology were also created by utilizing the CHARMM-36 force field. The protein was defined as being 1.5 nm from the box's edge in all directions, and the SPC water molecules were then placed inside the prescribed dodecahedron box. Further, it is balanced by adding opposite Cl^- ions. By steepest descent minimization algorithm, the simulated system was put through 500 steps of energy minimization. Equilibration of ions as well as solvents was done in two restricted phases. The NVT (isothermalisochoric) ensemble with a reference temperature of 310 K was then adjusted for 1 ns, followed by the NPT (isothermal-isobaric) ensemble with a reference pressure of 1.0 bar. Finally, systems that had been equilibrated were put through a production run of 100 ns.

Ergosterol extraction and estimation assay

A 100 µL of *C. albicans* from SDB was used to inoculate 10 mL of SDB for the test culture medium in a test tube. The Probe II was added at concentration of 1× and 2× MIC followed by fluconazole used as a positive control in separate test tubes. The fungal culture was incubated for 16 h and the cell pellets were separated by centrifugation at 5000 rpm for 10 mins. The total weight of the fungal cell pellet was measured. The alcoholic potassium hydroxide solution 25% (3 mL) was added to each pellet and mixed well for 1 min using vortex mixer. The cell suspensions were transferred to sterile screw-cap test tubes and incubated at 85 °C in water bath for 1 h. After incubation, the tubes were allowed to cool. The total sterols content was then extracted by addition 1 mL of sterile distilled water and 3 mL of *n*-heptane followed by vigorous vortex mixing for 3 mins. The solvent layer (heptane) was transferred to a screw-cap tube and stored at − 20 °C for the further use. To analyze the ergosterol content, 20 µL aliquot of sterol extract was diluted fivefold in 100% ethanol and absorption spectrum was measured at 295 nm using spectrophotometer (UV–Vis Spectrophotometer). To determine the

ergosterol content, Breivik and Owades (1957) outlined a method that involves calculating it as a percentage of the wet weight of the cell.

ADMET prediction analysis

To determine ADMET characteristics such as absorption, distribution, metabolism, excretion, toxicity, and physicochemical properties of all chemicals, the online prediction website ADMET lab 2.069 was used. Drug resemblance characteristics were found using the Lipinski rule of five in pkCSM (https://biosig.lab.uq.edu.au/pkcsm/prediction) and ADMET lab 2.0 (https://admetmesh.scbdd). The probe II was changed to SMILES format using Chemdraw Ultra; also, SMILES format was then posted to the pkCSM and ADMET lab 2.0 web servers. In addition, it makes it simpler to design the appropriate structures using the JMSE editor. When SMI structure was loaded, the data were submitted using the submit button, which generated ADMET characteristics as pdf that were downloaded and tabulated.

Results

Imidazo molecules

The imidazo[1,2-a]pyridine moieties play a vital role in pharmaceutical industries, medicinal chemistry and in various domains such as virology, endocrinology and cancer biology. Future therapeutic applications for novel imidazo[1,2-a]pyridines are possible (Enguehard-Gueiffier and Gueiffier 2007), and a viable strategy for creating medicinal compounds with new therapeutic indications involves using current medicines (Juárez-López and Schcolnik-Cabrera 2021). Here, we examined the antifungal and antibacterial properties of a newly synthesized novel imidazo[1,2-a]pyridines (Fig. 1) (Mala et al. 2019).

Antimicrobial activity

Two synthesized imidazole molecules (Probes I and II) were tested against a panel of Gram-positive, Gram-negative and fungal pathogens to check their antimicrobial potential. As depicted in Table 1, both the probes had no effect against *E. faecalis* and *E. coli*, whereas Probe II had better activity against *P. aeruginosa* with the highest concentration. Probe II exhibited an excellent zone of inhibition zone against *C. albicans* with a maximum inhibition zone (30.5 ± 0.7 mm at 200 µg) compared with Probe I (15.5 ± 0.7 at 200 µg) (Fig. 2) (Fig. S1a and 1b).

Minimum inhibitory concentration (MIC) of human pathogens

The MIC of Probes I and II against the Gram-positive, Gram-negative and fungal pathogens strains are presented in Table 2. Among the tested bacterial and fungal strains, the most susceptible was found against fungal pathogens *C. albicans*, with MIC values ranging between 7.50 and 15.01 µM/L for Probe II and Probe I show 454.93 µM/L, respectively. Probe I showed the highest activity against *P. aeruginosa* 454.93 µM/L for bacterial pathogens and Probe II shows 240.29 µM/L for *E. coli* and *P. aeruginosa*, respectively. Overall, Probe II demonstrated the highest activity against *C. albicans* at 15.01 µM/L (Table 2, Fig. S2).

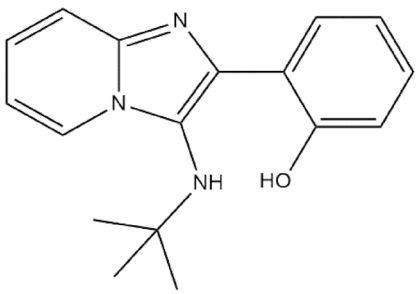

2-(3-(*tert*-butylamino)imidazo[1,2-*a*]pyridin-2-yl)phenol

Probe I

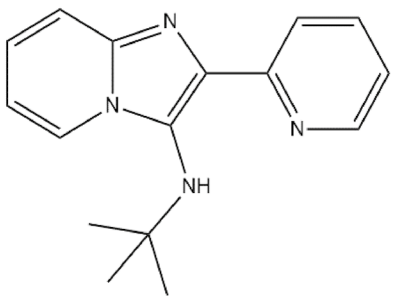

N-(*tert*-butyl)-2-(pyridin-2-yl)imidazo[1,2-*a*]pyridin-3-amine

Probe II

Fig. 1 Chemical structure of imidazo[1,2-a]pyridine derivatives

Table 1 Antimicrobial activity Probe I

Probe	Concentration	Antibacterial ZOI (mm)[a]			Antifungal ZOI (mm)[a]
		Gram positive	Gram negative		
		E. faecalis	*E. coli*	*P. aeruginosa*	*C. albicans*
I	100 µg/well	0	0	10.5 ± 0.7	0
	150 µg/well	0	0	11 ± 0	14.5 ± 0.7
	200 µg/well	0	0	12 ± 1.4	15.5 ± 0.7
II	100 µg/well	0	0	13.5 ± 0.7	25.5 ± 0.7
	150 µg/well	0	0	15 ± 0.7	28.5 ± 0.7
	200 µg/well	0	0	15.5 ± 0.7	30.5 ± 0.7

ZOI zone of inhibition

[a]Mean ± standard deviation

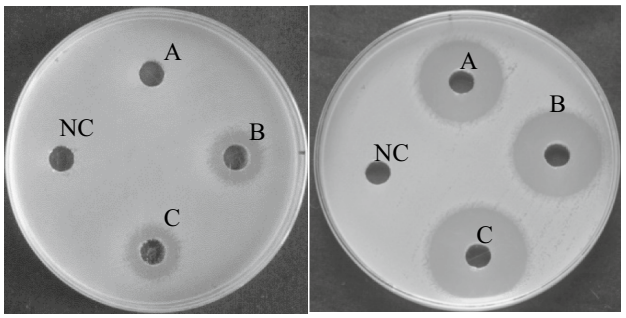

Fig. 2 Antifungal activity of Probes I and II

Potential of anti-candidal activity of Probe II against multidrug-resistance *Candida* spp.

Based on preliminary screening, the Probe II found to be a potential source against *Candida* spp. Further to identify its potential against different multidrug-resistance *Candida* spp. Probe II exhibited better antifungal activity against all selected *Candida* spp. compared with commercial antifungal drugs (Table 3). Among the 10 different clinical isolates, the zone of inhibition ranged between 12.5 and 18.5 mm at 40 µg per disk concentration (Fig. 3, Table 3, Fig. S3).

Minimum inhibitory concentration (MIC) and minimum fungicidal concentration (MFC) of Probe II

The MIC for Probe II was observed at 15.01 µM/L concentration against three clinical isolates, namely C5, C8 and C10 followed by 30.03 µM/L concentrations against six isolates, namely C1, C2, C3, C6, C7, and C9, whereas the MFC was 15.01 µM/L against C5, C8 and C10 followed by 30.03 µM/L. Comparatively, the Probe II was effectively inhibiting the growth and kills the fungal cell at the lowest concentration µM/L and µg/mL against C5, C8, and C10 clinical isolates (Table 4) (Fig. S4a–c 5).

Mechanism studies of anti-candidal activity

It is well known that the virulence of *Candida* depends on its transition from the yeast form to filamentous hyphae (Sionov et al. 2020). Multiphoton confocal microscopic observation of fungal mycelium treated with Probe II showed 95% of cell death after treatment and the inhibition of mycelia formation was observed (Fig. 4) At 1 h of exposure, more than 75% of cells, and after 8 h, 95% of cell death was observed.

Table 2 Minimum inhibitory concentration MIC of synthesized organic compounds

Molecules	Minimum inhibitory concentration (MIC) (µM/L)							
	Gram-positive bacterium		Gram-negative bacterium				Fungal pathogen	
	VREF		*E. coli*		*P. aeruginosa*		*C. albicans*	
	Probe	PC	Probe	PC	Probe	PC	Probe	PC
Probe I	909.87	4	909.87	4	454.93	2	454.93	NA
Probe II	1,922.35	2	240.29	8	240.29	4	15.01	NA

NA not appeared

Table 3 Antifungal activity of Probe II against multidrug-resistance *Candida* spp.

S. no	Pathogens	Esomeprazole	Fluconazole	Ketoconazole	Probe II (ZOI ± SD)	Control
1	C1	NA	NA	NA	13.5 ± 0.7	NA
2	C2	NA	NA	NA	14.5 ± 0.7	NA
3	C3	NA	NA	NA	14 ± 0.7	NA
4	C4	NA	NA	NA	12.5 ± 0.7	NA
5	C5	NA	NA	NA	18.5 ± 0.7	NA
6	C6	NA	NA	NA	14.5 ± 0.7	NA
7	C7	NA	NA	NA	14.5 ± 0.7	NA
8	C8	NA	NA	NA	16.5 ± 0.7	NA
9	C9	NA	NA	NA	15.5 ± 0.7	NA
10	C10	NA	NA	NA	17.5 ± 0.7	NA

NA not appeared; *ZOI* zone of inhibition

Fig. 3 Antifungal activity of Probe II

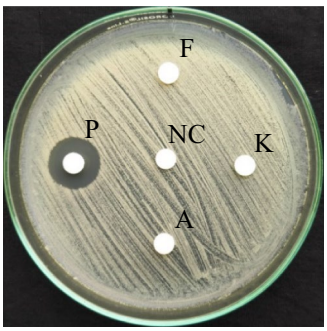

F: Fluconazole; K: Ketoconazole; A: Amphotericin B; P: Probe II; NC: Negative control

Table 4 The minimum inhibitory and minimum fungicidal concentration of Probe II against multidrug-resistance *Candida* sp.

S.no	Pathogens	Esomeprazole		Fluconazole		Ketoconazole		Probe II (μM/L)	
μg/mL		MIC	MFC	MIC	MFC	MIC	MFC	MIC	MFC
1	C1	ND	ND	ND	ND	ND	ND	30.03	60.07
2	C2	ND	ND	ND	ND	ND	ND	30.03	120.14
3	C3	ND	ND	ND	ND	ND	ND	30.03	60.07
4	C4	ND	ND	ND	ND	ND	ND	60.07	60.07
5	C5	ND	ND	ND	ND	ND	ND	15.01	15.01
6	C6	ND	ND	ND	ND	ND	ND	30.03	30.03
7	C7	ND	ND	ND	ND	ND	ND	30.03	60.07
8	C8	ND	ND	ND	ND	ND	ND	15.01	15.01
9	C9	ND	ND	ND	ND	ND	ND	30.03	60.07
10	C10	ND	ND	ND	ND	ND	ND	15.01	15.01

ND Not determined

In addition, no mycelial formation was observed in treated cells, whereas in untreated cells, the mycelial formation was observed after 4 h of culture growth (Fig. S5).

Hemolytic activity of Probe II

To determine the hemolytic activity of the Probe II, a standard hemolysis assay was performed. These results showed that there is no significant increase in hemolysis compared to negative control, with a maximum hemolysis of 0.45% observed at 512 μg/mL. Thus, the findings suggest that the Probe II has no ability to disrupt red blood cell membranes and cause hemolysis even at higher concentration. Further studies are needed to be explored on different human cells for its toxicity studies (Fig. 5, Table 5).

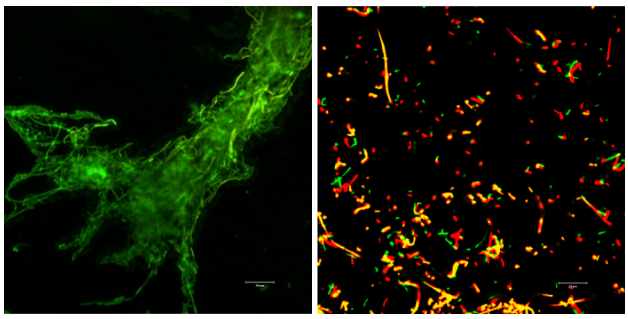

Fig. 4 Confocal microscopic observation of mycelial formation of *C. albicans*

Molecular docking Probe II with CYP51 by AutoDock tool 4.2

Molecular docking model of Probe II was carried out for CYP51 (PDB ID:5TZ1) inhibitor. On the basis of their interactions with the corresponding active residues and binding energies, a hundred conformations produced by a complex and the cluster confirmations along with the outcomes have been investigated. The binding clusters of Probe II with CYP51 complex had highest binding energy of − 7.59 kcal/mol, whereas pi–alkyl interactions were noted for Piperidine and imidazole rings of Probe II with B″ helical turn of CYP51 as illustrated in Fig. 6. In addition, this complex formed vdW contact with PHE228, LEU300, GLY303,

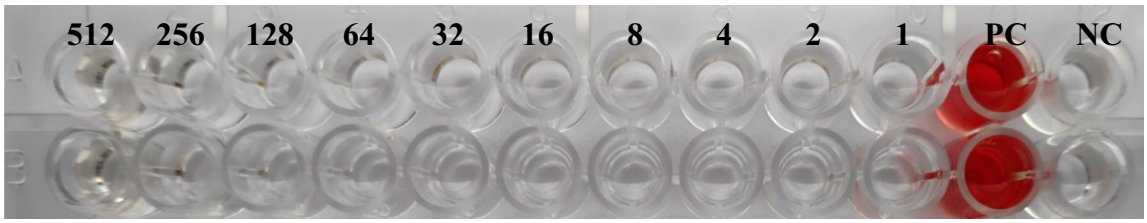

Fig. 5 Hemolytic activity of Probe II

Table 5 Percentage of hemolytic activity of Probe II

Con. µg/mL	512	256	128	64	32	16	8	4	2	1
Probe II	0.45 ± 0.63	0	0	0	0	0	0	0	0	0

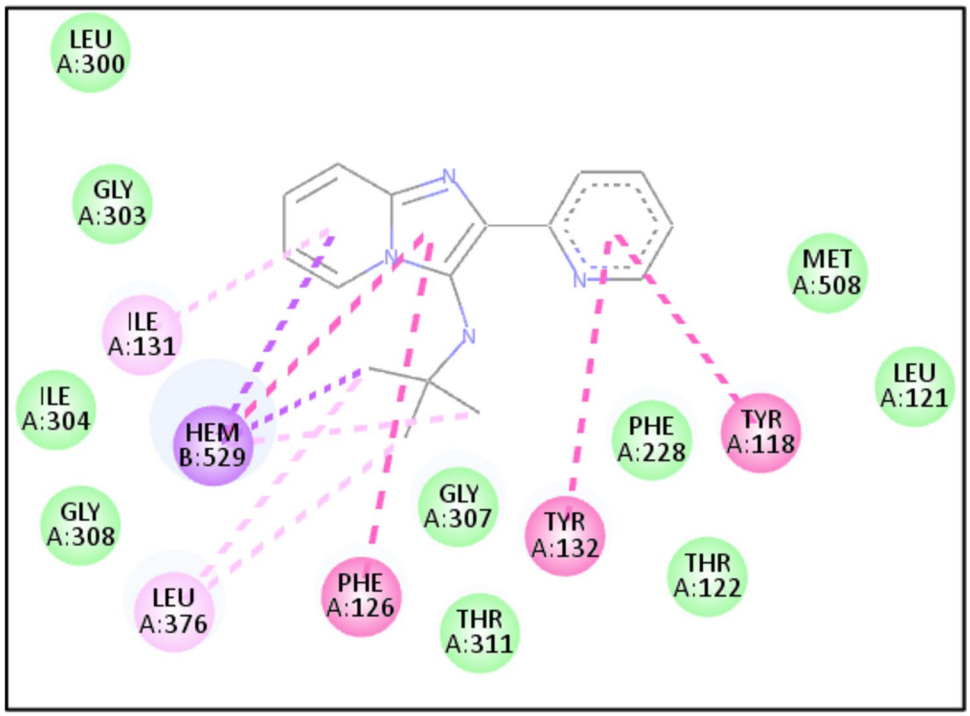

Fig. 6 Molecular docking of Probe II with CYP51 protein

Table 6 The essential residues and binding pocket of the CYP51 protein with probe 2

Complex	Binding pockets	Attributes	Residues
Probe 2–CYP51	Helix B′	Pi–alky/vdW/pi–sigma	TYR118, LEU121, THR122 and PHE126
	B″ helical turn	Pi–alky/vdW	VAL130, ILE131 and TYR132 PHE228 and PHE233, GLY303, ILE304, GLY307,
	Helix F″	vdW/pi–sigma	HIS310 and THR311
	Helix I	vdW	LEU376 and SER378
	K/β1–4 loop	Pi–alky/vdW/pi–sigma	MET508 and VAL509
	β4 hairpin	Pi–alky/vdW	

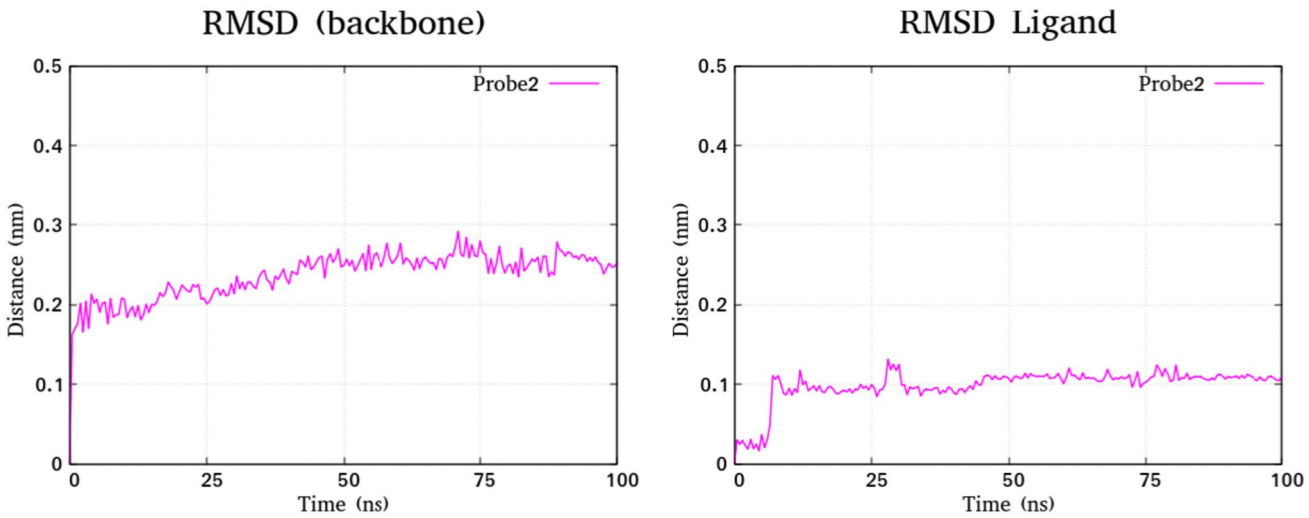

Fig. 7 As a function of time, (**A**) and (**B**), respectively, show the RMSD of the protein (CYP51) and probe 2

ILE304, GLY307, GLY308, THR311, LEU121, THR122 and MET508 from the Helix B′, Helix F″, Helix I, K/β1–4 loop, and β4 hairpin pockets, respectively (Table 6).

Molecular dynamics simulations of probe 2 with CYP51

We have predicted the dynamics and stability of Probe II–CYP51 complex. We executed 100 ns MD simulations for that complex using GROMACS. Following the procedure, complex output trajectories were analyzed to explore the simulation's numerous properties notably, radius of gyration, RMSD and RMSF(Rg). In initial MD simulation, the RMSD values of probe II–CYP51 complex were observed near to 0.22−0.29 nm having a mean RMSD of 0.23 nm as depicted in Fig. 7A, while that of ligand RMSD were discovered to be 0.09−0.13 nm having a mean RMSD of 0.09 nm which is shown in Fig. 7B. These RMSD regions have made sure that the complex is stable without experiencing significant changes in the protein's orientation. The computed RMSF value of this complex falls between 0.30 and 0.55 nm with an average of 0.15 nm. It has fluctuations at the end of the loop area, which is common in MD simulations (Fig. 8).

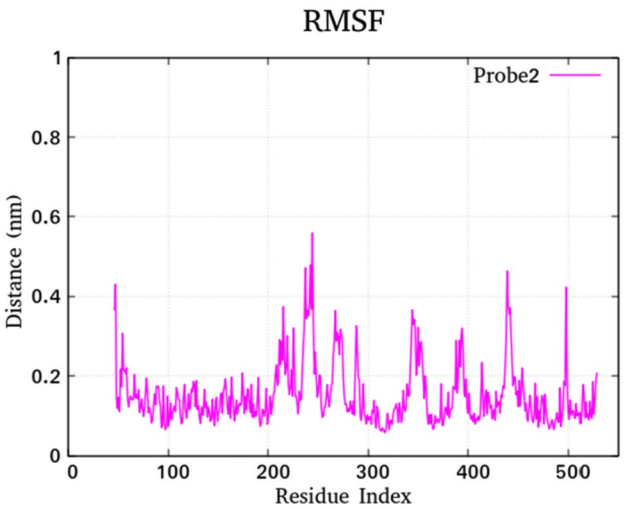

Fig. 8 The RMSF of CYP51 with probe 2 complex

The outcomes of our three MD simulations were combined and it was revealed that the probe II–CYP51 complex had the minimal RMSD values for the protein backbone and ligand and exhibited nearly imperceptible variations.

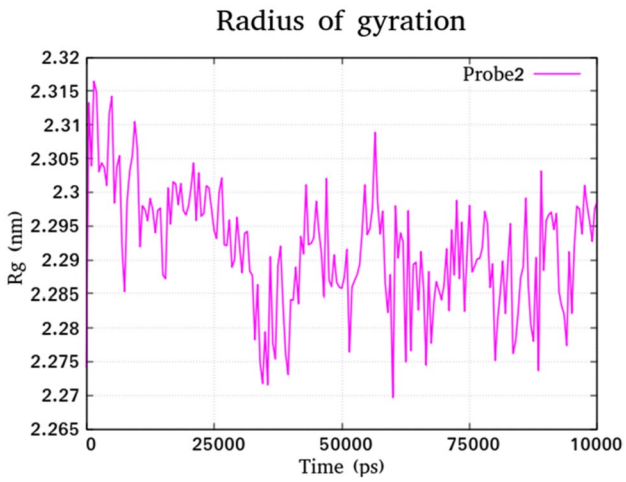

Fig. 9 Gyratory radius of CYP51 with probe II complex

Unexpectedly, the location of these fluctuations outside the binding cavity suggests that they had no effect on the overall hardness, flexibility and the integrity of the complex. The complex had minute differences in their gyration radii, confirming the general compactness of protein–ligand complex, which is illustrated in Figs. 8 and 9.

Validation of probe 2 with CYP51 protein binding by molecular dynamics simulations

The binding action of the probe II–CYP51 complex at the time intervals of 0, 25, 50, 75 and 100 ns were then interpreted, as shown in Fig. 10. The key residues and binding pockets of the CYP5 with the probe II are listed in Table 7.

The crystal structure of CYP51 had a number of binding pockets, including Helix B′, B″ helical turn, Helix F″ Helix I, K/β1–4 loop and β4 hairpin as illustrated in Table 7. Helix B′ binding pocket residues TYR118, LEU121, THR122 and PHE126 occurred pi–alkyl stacking, vdW and pi–sigma interaction with probe II around the MD simulation. The B″ helical turn binding pocket residues such as VAL130, ILE131 and TYR132 formed pi–alkyl and vdW contacts with probe II at 0 ns to 100 ns of MD simulation, whereas TYR132 residue created pi–alkyl contact at the beginning of the MD process, and then it made vdW contact at 25–100 ns. During the MD simulation, Helix I' binding pocket residues GLY303, ILE304, GLY307, HIS310 and THR311 were maintained via VDW with probe II. The K/β1–4 loop binding pocket contained the residues LEU376 and SER378, which were involved in the pi–alkyl, vdW and pi–sigma interactions with probe II throughout the MD. β4 hairpin binding pocket residues of

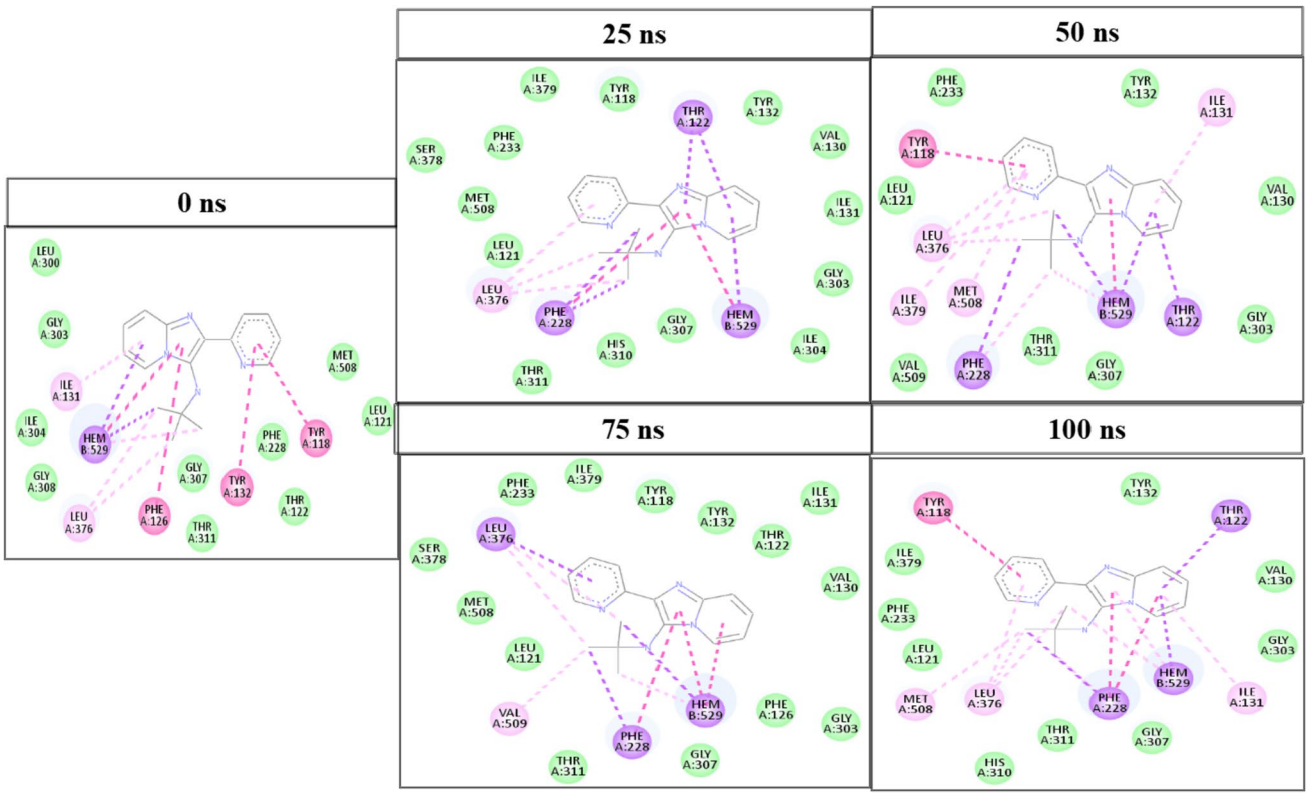

Fig. 10 Binding action of probe II–CYP51 complex with different intervals of MD simulations

Table 7 The probe II–CYP51 was interacted with the vdW (green), pi–alkyl (pink) and pi–sigma (purple) contacts around the binding residues of the proteins during 0–100 ns of MD simulations

CYP51-Probe2				
0 ns	25 ns	50 ns	75 ns	100 ns
TYR118	TYR118	TYR118	TYR118	TYR118
LEU121	LEU121	LEU121	LEU121	LEU121
THR122	THR122	THR122	THR122	THR122
PHE126			PHE126	
	VAL130	VAL130	VAL130	VAL130
ILE131	ILE131	ILE131	ILE131	ILE131
TYR132	TYR132	TYR132	TYR132	TYR132
PHE228	PHE228	PHE228	PHE228	PHE228
	PHE233	PHE233	PHE233	PHE233
LEU300				
GLY303	GLY303	GLY303	GLY303	GLY303
ILE304	ILE304			
GLY307	GLY307	GLY307	GLY307	GLY307
GLY308				
	HIS310			HIS310
THR311	THR311	THR311	THR311	THR311
LEU376	LEU376	LEU376	LEU376	LEU376
	SER378		SER378	
	ILE379	ILE379	ILE379	ILE379
MET508	MET508	MET508	MET508	MET508
		VAL509	VAL509	

CYP51 such as MET508 and VAL509 were made to interact with probe II through vdW and pi–sigma interactions at 0–100 ns of the MD simulation (Fig. 10).

Inhibition of ergosterol biosynthesis

Total sterol content of cells from *C. albicans* treated with Probe II at varying concentrations was studied. At 1× and 2× MICs, Probe II showed % ergosterol inhibition in *C. albicans*, at the concentration. The potential link between growth inhibition and the concentration of ergosterol in *C. albicans* was investigated using two treatments (Probe II and fluconazole as the control). The absorption spectra of the control exhibited four distinct peaks characteristic of sterols (Fig. 11). The Probe II at 1× and 2× concentrations caused reduced ergosterol levels of the yeast cells.

The absorption peak at 285 nm was used to quantify the ergosterol concentration, allowing for the calculation of the percentage of inhibition of its synthesis. Compared to fluconazole, the Probe II shows the greater percentage of inhibition (Probe II at 1× MIC 93.44%, 2× MIC 99%

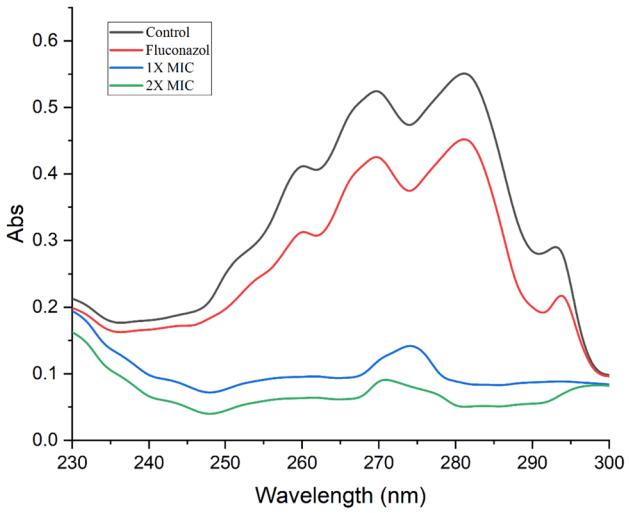

Fig. 11 Effect of probe II on the concentration of ergosterol synthesis in *Candida* sp

and fluconazole 11%) of ergosterol in the yeasts (Fig. 12). This result suggests that the target site of probe to could effectively bind with sterol 14-alpha demethylase (CYP51) from Candida albicans stage of the ergosterol biosynthetic pathway.

ADMET properties

Lead optimization heavily relies on the identification of biochemical action of Probe II from drug delivery to elimination. The majority of synthesized compounds exhibit great pharmacological action, and yet few are generally unaccepted majorly because of its weak absorption, distribution, metabolism, excretion, and toxicity (ADMET) properties (Bodedla et al. 2015). The newly developed drug candidate should be non-toxic, effectively given, and absorbed into

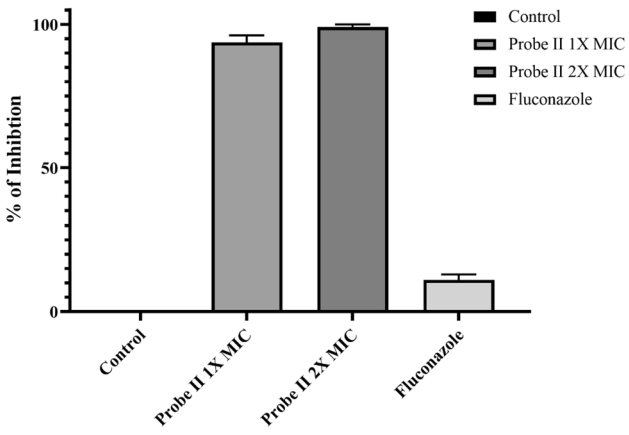

Fig. 12 Percentage of ergosterol inhibition

systemic circulation without impairing biological activity. The assessment of ADMET characteristics is crucial in the drug development process even though these methods appear to be distinct from one another. Therefore, using the online tool ADMETlab 2.0, the physicochemical characteristics, ADME and for Probe II, and medicinal properties of probe II were calculated. Physical and chemical characteristics, Caco-2 permeability, human intestinal absorption, blood–brain barrier (BBB) permeability, P-glycoprotein substrate, respiratory toxicity, eye corrosion, eye irritation, AMES toxicity, plasma protein binding, ClearanceMDCK permeability, Half-life ($T_{1/2}$), carcinogenicity, and synthetic accessibility were taken into account when determining the ADME factors. In expressions of Human Intestinal Absorption (HIA), it was found that all substances had positive calculated values, indicating that they can more readily pass through the intestinal barrier. The Probe II had higher PPB values (95.05%) in this investigation found to be low therapeutic index though the further in-vitro study may help to find the complete toxicity. The BBB and blood placental barriers (BPB) were exposed to moderate probability of being BBB positive. The fraction unbound (Fu) is found to be very low as 3.039%. The metabolism of Probe II shows values 0.119–0.981 property for CYP1A2 inhibitor, CAP1A2 substrate, and CYP2C19 inhibitor. The excretion property of Probe II show the clearance (CL) is 4.085 mL/min/kg $T_{1/2}$ found as 0.528 (Supplementary Table 1).

Discussion

Imidazopyridine is one of the important fused bicyclic 5–6 heterocycles and it is recognized as a "drug prejudice" scaffold due to its wide range of applications in medicinal chemistry (Bagdi et al. 2015) and it is an important target in organic synthetic chemistry and have attracted the critical attention of chemists mainly due to the discovery of the interesting properties exhibited by a great number of imidazo[1,2-*a*]pyridine derivatives. Although lot of synthetic methods of imidazo[1,2-*a*]pyridines have been developed in the past years, the chemistry community faces continuing challenges to use green reagents, maximize atom economy and enrich the functional group diversity of products. Undoubtedly, with its low cost and lack of environmentally hazardous byproducts, cascade reactions and C–H functionalization are ideal strategies for this field. In this record, we highlight some of our progress towards the goal to synthesis of imidazo[1,2-*a*]pyridine derivatives through carbene transformations or C–H functionalizations (Yu et al. 2019). Candidiasis is a major health problem where Candida spp. forms biofilm on endothelial and epithelial cells. In immunosuppressed people, it can lead to systemic infection and even death. The oral cavity, the genitourinary tract, and the intestine are the most frequent infection sites. It is important to find treatments that can interfere with the early adhesion of the fungi to the host cells (Sionov et al. 2020). The imidazo[1,2-a]pyridines derivatives have excellent activity against herpesviruses, cytomegalovirus (Gudmundsson and Johns 2007), cytomegalovirus and/or varicella-zoster virus, and Human Rhinovirus. The imidazo[1,2-a]pyridine also acts as antifungal as well as anthelmintic agents, the promising drug candidate for antitumor therapy, antiulcer agents, *M. tuberculosis* and *M. bovis*, anticonvulsant studies, antiprotozoal agents, analgesic and anti-inflammatory properties (Gueiffier et al. 1996; Goel et al. 2016; Abrahams et al. 2012). In a study, 34 imidazole derivatives were screened for their antimicrobial potential among them five compounds found to be highly potential against all tested fungal stains, namely *Saccharomyces cerevisiae*, *Candida albicans* and *Candida krusei* (Bouchal et al. 2019). Likewise, another study found that three azole compounds revealed excellent antimicrobial activity against all Gram-positive and Gram-negative bacteria, and the fungal *A. flavus*, while moderate activity against *C. albicans*; six compounds displayed higher activities against Gram-positive bacteria (*S. aureus* and *B. subtilis*) and the Gram-negative *P. aeruginosa* (Hashem et al. 2020). As discussed earlier, the imidazole molecules possess wide range of microbial activity. However, in this present study, we found that imidazo[1,2-a]pyridine derivative possesses excellent anti-candidal activity rather than the bacterial activity.

The mechanism of action of triazoles is based on the inhibition of the microsomal cytochrome P450 (CYP450) monooxygenase-dependent 14-α-demethylase. The demethylation of fungal lanosterol is a two-step process involving the reduced form of nicotinamide dinucleotide phosphate (NADPH) and oxygen. As nitrogen from the triazole ring binds to the heme iron, oxidation of the methyl group is prevented. The combination of the accumulation of toxic 14-α-methylsterols and depletion of ergosterol results in the fungistatic effect (Sagatova et al. 2015).

Conclusion

The antifungal effects of imidazo[1,2-a]pyridine derivatives were investigated and it was found to effectively inhibit the growth and proliferation of different fungal strains, including drug-resistant *Candida* spp. In fact, a minimum inhibitory concentration of 4 µg/mL proved sufficient in eradicating these fungal pathogens. Moreover, the in-silico analysis demonstrates that Probe II exhibits strong binding affinity to the target site of sterol 14-alpha demethylase inhibitors from *C. albicans*. It has been observed that Probe II effectively inhibits ergosterol formation. Preliminary cell-based assays have shown that minimal toxicity towards human

blood samples and ADMET analysis indicates moderate compatibility across all the categories. These findings suggest a potential application for this new imidazole derivative in topical treatment for Candidal infections and contribute to ongoing research on the development of novel antifungal medications.

Supporting information

Additional figures all well diffusion photos, Minimum inhibitory concentration and hyphal formation inhibition from Candida are presented in PPT. Accession Codes: PDB code for Sterol 14-alpha demethylase (CYP51) protein from *C. albicans* is 5TZ1.

Supplementary Information The online version contains supplementary material available at https://doi.org/10.1007/s00203-023-03780-w.

Acknowledgements I sincerely acknowledge Dr. Jayapraksh priya BCMML, CAS in Botany, University of Madras for providing the fungal culture. I would like to acknowledge research scholar for BCMML, CAS for their help with data collection.

Author contributions MN: design, research finding and experimental works; RM: molecule synthesis; KS: molecular docking and dynamics; DD: writing chemistry part; MN: framed experimental design and methodology; PV: study of inhibition of ergosterol biosynthesis; MMS: writing and correcting the manuscript.

Funding Not applicable.

Data availability The data that support the findings of this study are available on request from the corresponding author Dr. Manivannan Nandhagopal.

Declarations

Conflict of interest The authors declare no competing interests.

Consent for publication Not applicable.

References

Abrahams KA, Cox JAG, Spivey VL et al (2012) Identification of novel imidazo[1,2-a]pyridine inhibitors targeting *M. tuberculosis* QcrB. PLoS ONE 7:e52951

Alabi PE, Gautier C, Murphy TP et al (2023) Small molecules restore azole activity against drug-tolerant and drug-resistant Candida isolates. Mbio 14(4):e0047923

Bagdi AK, Santra S, Monir K, Hajra A (2015) Synthesis of imidazo[1,2-a]pyridines: a decade update. Chem Commun 51:1555–1575

Bar-Yosef H, Vivanco Gonzalez N, Ben-Aroya S, Kron SJ, Kornitzer D (2017) Chemical inhibitors of Candida albicans hyphal morphogenesis target endocytosis. Sci Rep 7:5692

Bodedla GB, Justin Thomas KR, Kumar S, Jou J-H, Li C-J (2015) Phenothiazine-based bipolar green-emitters containing benzimidazole units: synthesis, photophysical and electroluminescence properties. RSC Adv 5:87416–87428

Bouchal B, Abrigach F, Takfaoui A et al (2019) Identification of novel antifungal agents: antimicrobial evaluation, SAR, ADME-Tox and molecular docking studies of a series of imidazole derivatives. BMC Chem Biol 13:100

Breivik ON, Owades JL (1957) Yeast analysis, spectrophotometric semimicrodetermination of ergosterol in yeast. J Agri Food Chem 5(5):360–363

Bruder-Nascimento A, Camargo CH, Mondelli AL, Sugizaki MF, Sadatsune T, Bagagli E (2014) Candida species biofilm and *Candida albicans* ALS3 polymorphisms in clinical isolates. Braz J Microbiol 45:1371–1377

Chin VK, Lee TY, Rusliza B, Chong PP (2016) Dissecting *Candida albicans* infection from the perspective of *C. albicans* virulence and omics approaches on host–pathogen interaction: a review. Int J Mol Sci 17(10):1643. https://doi.org/10.3390/ijms17101643

Cui X, Wang L, Lü Y, Yue C (2022) Development and research progress of anti-drug resistant fungal drugs. J Infect Public Health 15:986–1000

Daneshnia F, de Almeida Júnior JN, Ilkit M et al (2023) Worldwide emergence of fluconazole-resistant *Candida parapsilosis*: current framework and future research roadmap. Lancet Microbe 4:e470–e480

de Oliveira Santos GC, Vasconcelos CC, Lopes AJO et al (2018) Candida infections and therapeutic strategies: mechanisms of action for traditional and alternative agents. Front Microbiol 9:1351

Enguehard-Gueiffier C, Gueiffier A (2007) Recent progress in the pharmacology of imidazo[1,2-a]pyridines. Mini Rev Med Chem 7:888–899

Goel R, Luxami V, Paul K (2016) Imidazo[1,2-a]pyridines: promising drug candidate for antitumor therapy. Curr Top Med Chem 16:3590–3616

Gudmundsson KS, Johns BA (2007) Imidazo[1,2-a]pyridines with potent activity against herpesviruses. Bioorg Med Chem Lett 17:2735–2739

Gueiffier A, Lhassani M, Elhakmaoui A et al (1996) Synthesis of acyclo-C-nucleosides in the imidazo[1,2-a]pyridine and pyrimidine series as antiviral agents. J Med Chem 39:2856–2859

Hashem HE, Amr AE-GE, Nossier ES, Elsayed EA, Azmy EM (2020) Synthesis, antimicrobial activity and molecular docking of novel thiourea derivatives tagged with thiadiazole, imidazole and triazine moieties as potential DNA gyrase and topoisomerase IV inhibitors. Molecules 25:2766. https://doi.org/10.3390/molecules25122766

Iyer KR, Robbins N, Cowen LE (2022) The role of Candida albicans stress response pathways in antifungal tolerance and resistance. iScience 25:103953

Juárez-López D, Schcolnik-Cabrera A (2021) Drug repurposing: considerations to surpass while re-directing old compounds for new treatments. Arch Med Res 52:243–251

Kamli MR, Srivastava V, Hajrah NH et al (2021) Facile bio-fabrication of Ag–Cu–Co trimetallic nanoparticles and its fungicidal activity against *Candida auris*. J Fungi (basel) 7:62. https://doi.org/10.3390/jof7010062

Mahmoud DE, Faraag AHI, Abu El-Wafa WM (2021) In vitro study on the potential fungicidal effects of atorvastatin in combination with some azole drugs against multidrug resistant *Candida albicans*. World J Microbiol Biotechnol 37:191

Mala R, Suman K, Nandhagopal M (2019) Chelation of specific metal ions imparts coplanarity and fluorescence in two imidazo [1, 2-a] pyridine derivatives: potential chemosensors for detection of metal ions in in aqueous and biosamples. Spectrochim Acta A Mol Biomol Spectrosc 222:117236

Mayer FL, Wilson D, Hube B (2013) *Candida albicans* pathogenicity mechanisms. Virulence 4:119–128

Odds FC (1993) Resistance of yeasts to azole-derivative antifungals. J Antimicrob Chemother 31:463–471

Panda SK, Buroni S, Tiwari V, Nascimento da Silva LC (2021) Editorial: insights into new strategies to combat biofilms. Front Microbiol 12:742647

Rahimi-Verki N, Shapoorzadeh A, Razzaghi-Abyaneh M et al (2016) Cold atmospheric plasma inhibits the growth of *Candida albicans* by affecting ergosterol biosynthesis and suppresses the fungal virulence factors in vitro. Photodiagn Photodyn Ther 13:66–72

Sagatova AA, Keniya MV, Wilson RK, Monk BC, Tyndall JDA (2015) Structural insights into binding of the antifungal drug fluconazole to *Saccharomyces cerevisiae* lanosterol 14α-demethylase. Antimicrob Agents Chemother 59:4982–4989

Sionov RV, Feldman M, Smoum R, Mechoulam R, Steinberg D (2020) Anandamide prevents the adhesion of filamentous *Candida albicans* to cervical epithelial cells. Sci Rep 10:13728

Somarathinam K, Gunalan S, Sailapathi A et al (2023) Antihypertensive effects of pentacyclic triterpenoid from *Convolvulus pluricaulis* and its plausible mechanism of action hypothesizing its selectivity targeting mineralocorticoid receptor of RAAS. Phytomed plus 3:100408

Velusamy P, Das J, Pachaiappan R, Vaseeharan B, Pandian K (2015) Greener approach for synthesis of antibacterial silver nanoparticles using aqueous solution of neem gum (*Azadirachta indica L.*). Indus Crop Prod 66:103–109

Wang E, Farmakiotis D, Yang D et al (2015) The ever-evolving landscape of candidaemia in patients with acute leukaemia: non-susceptibility to caspofungin and multidrug resistance are associated with increased mortality. J Antimicrob Chemother 70:2362–2368

Yu Y, Su Z, Cao H (2019) Strategies for synthesis of imidazo[1,2-a] pyridine derivatives: carbene transformations or C–H functionalizations. Chem Rec 19:2105–2118

Zhao Y, Chan JF-W, Tsang C-C et al (2015) Clinical characteristics, laboratory identification, and in vitro antifungal susceptibility of Yarrowia (Candida) lipolytica isolates causing fungemia: a multicenter, prospective surveillance study. J Clin Microbiol 53:3639–3645

Authors and Affiliations

Manivannan Nandhagopal[1] · Ramanjaneyulu Mala[2] · Kanagasabai Somarathinam[3] · Divya Dhakshinamurthy[4] · Mathivanan Narayanasamy[5] · Priyadharshni Vijayan[5] · Manimuthu Mani Shankar[6]

✉ Manivannan Nandhagopal
micromani444@gmail.com

Ramanjaneyulu Mala
ramanjiclri@gmail.com

Kanagasabai Somarathinam
skanagu.sabai@gmail.com

Divya Dhakshinamurthy
divyadhakshinamurthy@gmail.com

Mathivanan Narayanasamy
prabhamathi@yahoo.com

Priyadharshni Vijayan
vpriyadharshni1988@gmail.com

[1] Bio-Control and Microbial Product Lab, Department of Microbiology, Saveetha Medical College and Hospital, Saveetha Institute of Medical and Technical Sciences, Thandalam, Chennai 602105, India

[2] Organic and Bioorganic Chemistry Laboratory, CSIR-Central Leather Research Institute, Adyar, Chennai 600020, India

[3] Centre for Advanced Studies in Crystallography and Biophysics, University of Madras, Guindy Campus, Chennai 600 025, Tamil Nadu, India

[4] Department of Chemistry, Vel Tech Rangarajan Dr, Sagunthala R&D Institute of Science and Technology, Avadi, Chennai 600062, India

[5] Biocontrol and Microbial Metabolites Lab, Centre for Advanced Studies in Botany, University of Madras, Guindy Campus, Chennai, Tamil Nadu, India

[6] Department of Biochemistry, Saveetha Medical College and Hospital, Saveetha Institute of Medical and Technical Sciences, Thandalam, Chennai 602105, India